

On Reflection and Refraction of the Laser Light Pulse at the Vacuum–Medium Interface

W Żakowicz^{1,*} and A. A. Skorupski^{2,†}

¹*Institute of Physics, Polish Academy of Sciences, Al. Lotników 32/46, 02–668 Warsaw, Poland*

²*Department of Theoretical Physics, National Centre for Nuclear Research, Hoża 69, 00–681 Warsaw, Poland*

(Dated: December 8, 2024)

By generalizing the well known results for reflection and refraction of plane waves at the vacuum–medium interface to Gaussian light beams, we obtain analytic formulas for reflection and refraction of the TM and TE laser light pulses. This enables us to give a possible explanation why no reflection was observed in light pulse photographs in some vicinity of the air–resin interface, given in L. Gao, J. Liang, C. Li, and L. V. Wang, *Nature* **516**, 74 (2014). We suggest how to modify the experimental setup so as to observe the reflected pulse.

PACS numbers: 42.25.Gy

In an impressive paper [1] describing ultrafast photography (10^{11} frames per second), among examples given there was a laser light pulse photograph in some vicinity of the vacuum–resin interface, see Fig. 3 b in [1]. The transmitted pulse could be seen there, but no reflected one was observed. Here we try to explain why there was no reflection, and how to modify the experimental setup to observe it.

We assume that in our laboratory Cartesian coordinate system (x, y, z) , with a medium at $y < 0$ and vacuum at $y > 0$, we can fulfill the boundary conditions at the interface, $y = 0$, by a superposition of three beams propagating in the x, y plane: the incident (i), reflected (r) and refracted (or transmitted, t) Gaussian beam. In the paraxial approximation, we can describe any such steady state TM beam as [2, 3] (Gaussian units)

$$H_{z_{i,r,t}} = C_{i,r,t} \exp \left[-\frac{x_{i,r,t}^2}{w_{x_{i,r,t}}^2} - \frac{z^2}{w_z^2} - i\omega \left(t - \frac{y_{i,r,t}}{c/n_{i,r,t}} \right) \right], \quad (1a)$$

$$E_{x_{i,r,t}} = -Z_{i,r,t} H_{z_{i,r,t}}, \quad (1b)$$

where $C_i = 1$, $C_r = R_{\text{TM}}$ is the reflection coefficient, $C_t = T_{\text{TM}}$ is the transmission coefficient, $y_{i,r,t}$ are Cartesian coordinates along each beam, $x_{i,r,t}$ are similar coordinates for the transverse direction, $n_{i,r} = 1$ and $n_t = n \equiv \sqrt{\epsilon\mu}$ are the refraction indexes of vacuum and medium, $Z_{i,r} = 1$ and $Z_t = \sqrt{\mu/\epsilon}$ are similar field impedances, and the constants ϵ and μ characterize the medium.

Note that the beam radii w_x and w_z are constant here (y independent). This requires y to be small as compared to the Rayleigh ranges \hat{y}_x and \hat{y}_z :

$$(y/\hat{y}_{x,z})^2 \ll 1, \quad \hat{y}_{x,z} = \pi w_{x,z}^2/\lambda, \quad (2)$$

where $\lambda = (c/n)2\pi/\omega$ is the wavelength, c is the speed of light in vacuum and ω is the angular frequency.

Note that by TM (or TE) polarization we mean the direction of the \mathbf{H} (or \mathbf{E}) vector with respect to the plane of incidence (x, y in our case).

In the limit $w_x \rightarrow \infty$ and $w_z \rightarrow \infty$ in (1), we obtain the plane waves: $H_z = C \exp[i(ky - \omega t)]$. Therefore in this limit, the continuity of the tangential components of \mathbf{E} and \mathbf{H} for the incident plus reflected beam versus the transmitted one at the interface ($y = 0$) implies the Snell law

$$\varphi_r = \varphi_i, \quad n \sin \varphi_t = \sin \varphi_i, \quad (3)$$

and the Fresnel formulas [3, 4] ($\nu = n \cos \varphi_t$)

$$R_{\text{TM}} = \frac{\epsilon \cos \varphi_i - \nu}{\epsilon \cos \varphi_i + \nu}, \quad T_{\text{TM}} = 1 + R_{\text{TM}}, \quad (4a)$$

$$R_{\text{TE}} = \frac{\mu \cos \varphi_i - \nu}{\mu \cos \varphi_i + \nu}, \quad T_{\text{TE}} = 1 + R_{\text{TE}}, \quad (4b)$$

where φ_i , φ_r and φ_t are the angles of incidence, reflection and refraction.

For finite radii $w_{x_{i,r,t}}$ and $w_z = w_{z_{i,r,t}}$, we have to take into account linear relations defining $x_{i,r,t}$ and $y_{i,r,t}$ as functions of the laboratory x and y ($z_{i,r,t} = -z$):

$$x_{i,r,t} = (x, y) \cdot \hat{\mathbf{x}}_{i,r,t}, \quad y_{i,r,t} = (x, y) \cdot \hat{\mathbf{y}}_{i,r,t}, \quad (5)$$

where hats denote unit vectors for local coordinate axes of each beam,

$$\hat{\mathbf{x}}_{i,r} = (\pm \cos \varphi_i, \sin \varphi_i), \quad \hat{\mathbf{x}}_t = (\cos \varphi_t, \sin \varphi_t), \quad (6)$$

$$\hat{\mathbf{y}}_{i,r} = (\sin \varphi_i, \mp \cos \varphi_i), \quad \hat{\mathbf{y}}_t = (\sin \varphi_t, -\cos \varphi_t). \quad (7)$$

At the boundary, $y = 0$, equations (5) lead to

$$\frac{x_{i,r}^2}{w_{x_{i,r}}^2} = x^2 \frac{\cos^2 \varphi_i}{w_{x_{i,r}}^2}, \quad \frac{x_t^2}{w_{x_t}^2} = x^2 \frac{\cos^2 \varphi_t}{w_{x_t}^2}. \quad (8)$$

Thus if $x = z = 0$, Eq. (1) is the same as that for plane waves, and the boundary conditions are satisfied. They will be satisfied also for nonzero x and z , if the RHS of (8) are the same, i.e., if

$$w_{x_r} = w_{x_i}, \quad w_{x_t} = w_{x_i} \frac{\cos \varphi_t}{\cos \varphi_i} > w_{x_i}. \quad (9)$$

For the TE Gaussian beam one has to replace TM \rightarrow TE, $H_{z_{i,r,t}} \rightarrow E_{z_{i,r,t}}$, and $H_{x_{i,r,t}} = E_{z_{i,r,t}}/Z_{i,r,t}$.

If the incident laser beam is not monochromatic, but has a spectrum function $F(\omega)$, we have to include all harmonics, and the time behavior will be given by the

integrals (Inverse Fourier Transforms)

$$\int_{-\infty}^{\infty} F(\omega) \exp\left(-i\omega\left(t - \frac{y_{i,r,t}}{c/n_{i,r,t}}\right)\right) d\omega. \quad (10)$$

For a Gaussian spectrum function centered about $\omega = \omega_0$,

$$F(\omega) = \exp\{-(\omega - \omega_0)/b\}^2\}, \quad (11)$$

the Gaussian wave packets will be obtained. In that case, for a conveniently normalized TM laser beam, we end up with (neglecting the common factor $b\sqrt{\pi}$):

$$H_z(y > 0) = \exp\left[-\frac{x_i^2}{w_{x_i}^2} - \frac{(y_i - ct)^2}{w_{y_i}^2} - \frac{z^2}{w_z^2} + ik_0(y_i - ct)\right] + R_{\text{TM}} \exp\left[-\frac{x_r^2}{w_{x_r}^2} - \frac{(y_r - ct)^2}{w_{y_r}^2} - \frac{z^2}{w_z^2} + ik_0(y_r - ct)\right], \quad (12)$$

$$H_z(y \leq 0) = (1 + R_{\text{TM}}) \exp\left[-\frac{x_t^2}{w_{x_t}^2} - \frac{(y_t - ct/n)^2}{w_{y_t}^2} - \frac{z^2}{w_z^2} + ik_0n(y_t - ct/n)\right], \quad (13)$$

where

$$w_{y_i} = 2c/b, \quad w_{y_r} = w_{y_i}, \quad w_{y_t} = w_{y_i}/n, \quad (14)$$

are the the light pulse radii along each beam, while $k_0 = 2\pi/\lambda_0$, $\lambda_0 = cT_0$ and $T_0 = 2\pi/\omega_0$ are the vacuum wavenumber, wavelength and period for the beam carrier, $\omega = \omega_0$. See also (5)–(7) and (9) for remaining definitions, in which $\varphi_t = \arcsin[(\sin \varphi_i)/n]$.

Replacing $H_z \rightarrow E_z$ and $R_{\text{TM}} \rightarrow R_{\text{TE}}$ in (12) and (13), we obtain the TE beam fields.

The real parts of the complex coordinates H_z and E_z defined above give us the z coordinates of the real physical fields.

From now on, it will be convenient to work with dimensionless variables, by measuring time and space dimensions in the units of T_0 and λ_0 , see Figs. 1–3. This implies $c = 1$ and $k_0 = 2\pi$ in (12) and (13).

At $t = 0$, for each of the pulses in (12) and (13), the real part is a product of a strongly oscillating function of $y_{i,r,t}$

($\cos(2\pi y_i)$, $\cos(2\pi y_r)$, or $\cos(2\pi n y_t)$), with wavelengths $\lambda_i = \lambda_r = 1$, $\lambda_t = 1/n$, and the envelope which is a Gaussian proportional to

$$\exp\left[-(\text{space coordinate}/\text{pulse radius})^2\right]. \quad (15)$$

During time evolution starting at some $t = t_{\text{in}} < 0$, the incident and reflected pulses move along the y_i and y_r axes with unit velocities, and the refracted pulse along the y_t axis with the velocity $1/n$.

Notice that there is a common factor $\exp(-z^2/w_z^2)$ in (12) and (13). Its square will appear as a common factor in formulas defining energy densities (time averaged over fast oscillations with $\omega = 2\omega_0$), $\mu H_z H_z^*$ and $\epsilon E_z E_z^*$. Integrating these formulas dz from $-\infty$ to ∞ we obtain (time averaged) surface energy densities, $\mathcal{E}_{\text{TM}}(x, y, t)$ and $\mathcal{E}_{\text{TE}}(x, y, t)$. Neglecting the common factor $w_z\sqrt{\pi}/2$, we end up with

$$\begin{aligned} \mathcal{E}_{\text{TM}}(x, y > 0, t) &= \exp\left[-\left(\frac{x_i}{w_{x_i}/\sqrt{2}}\right)^2 - \left(\frac{y_i - t}{w_{y_i}/\sqrt{2}}\right)^2\right] + R_{\text{TM}}^2 \exp\left[-\left(\frac{x_r}{w_{x_r}/\sqrt{2}}\right)^2 - \left(\frac{y_r - t}{w_{y_r}/\sqrt{2}}\right)^2\right] \\ &\quad + 2R_{\text{TM}} \exp\left[-\frac{x_i^2 + x_r^2}{w_{x_i}^2} - \frac{(y_i - t)^2 + (y_r - t)^2}{w_{y_i}^2}\right] \cos(4\pi y \cos \varphi_i), \end{aligned} \quad (16)$$

$$\mathcal{E}_{\text{TM}}(x, y \leq 0, t) = \mu(1 + R_{\text{TM}})^2 \exp\left[-\left(\frac{x_t}{w_{x_t}/\sqrt{2}}\right)^2 - \left(\frac{y_t - t/n}{w_{y_t}/\sqrt{2}}\right)^2\right]. \quad (17)$$

Replacing TM \rightarrow TE and $\mu \rightarrow \epsilon$ in (16) and (17) we

obtain formulas for $\mathcal{E}_{\text{TE}}(x, y, t)$. The free parameters are:

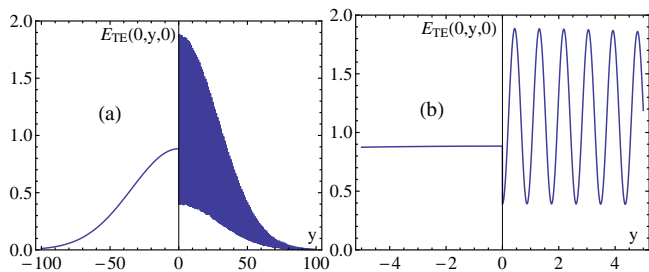


FIG. 1. (Color online) (a): $\mathcal{E}_{\text{TE}}(x=0, y, t=0)$ versus y . (b): Blowup demonstrating discontinuity in \mathcal{E}_{TE} due to discontinuity in ϵ at the interface ($y=0$), $\mathcal{E}_{\text{TE}}(y=0^-) = \epsilon \mathcal{E}_{\text{TE}}(y=0^+)$. This also demonstrates continuity of E_z at the interface.

φ_i , w_{x_i} and w_{y_i} .

In (16) and (17), one can recognize squares of the envelopes for the fields (12) and (13), which move along the same axes and with the same velocities as the fields ($v_{i,r} = 1$, and $v_t = 1/n$). The third term in (16) describes the interference of the incident and reflected pulses in vacuum. This term, different from zero when the incident and reflected pulses overlap, is strongly oscillating in the laboratory coordinate y , see Fig. 1. The wavelength (of standing wave)

$$\lambda_{\text{sw}} = \frac{1}{2 \cos \varphi_i} \quad (18)$$

depends on the angle of incidence φ_i but is independent of the pulse radii, i.e., independent of the incident beam radius w_{x_i} , and laser pulse duration $\tau_i = 2w_{y_i}/c$, where $c = 1$.

The parameters used in [1] were: $n = 1.5$ and $\mu = 1$, which implied $\epsilon = 2.25$. Furthermore, $\varphi_i = 55^\circ$ and $w_{y_i}/w_{x_i} = 2$, as we could read from Fig. 3b in [1]. The value of φ_i was close to the Brewster angle $\varphi_B \equiv \arctan n = 56.31^\circ$ for which $R_{\text{TM}} = 0$ ($R_{\text{TM}}^2(\varphi_i = 55^\circ) = 1.77847 \times 10^{-4}$). This could be the reason why no reflection was observed in [1], see Fig. 2, and would suggest the laser pulse to have TM polarization. In that case, by rotating the light source by 90° around the incident beam axis, the TE polarization would be obtained, for which $R_{\text{TE}}^2(\varphi_i = 55^\circ) = 0.1393$ versus $\epsilon(1 + R_{\text{TE}})^2 = 0.8840$ for the refracted beam. The reflected pulse should then be seen along with the incident and refracted ones, see Fig. 3.

In our calculations, based on the dimensionless formulas (16) and (17), we have chosen the pulse dimensions to be rather small: $w_{x_i} = 50$ and $w_{y_i} = 100$. The actual dimensions of the pulses used in [1] were much larger but, as we will see, the results in that case are closely related to ours.

Notice that at $t = 0$, except for the \cos in (16), all remaining terms and factors in (16) and (17) are of the form (15) (possibly with the replacement (pulse radius) \rightarrow (pulse radius)/ $\sqrt{2}$). Thus, if we multiply the incident

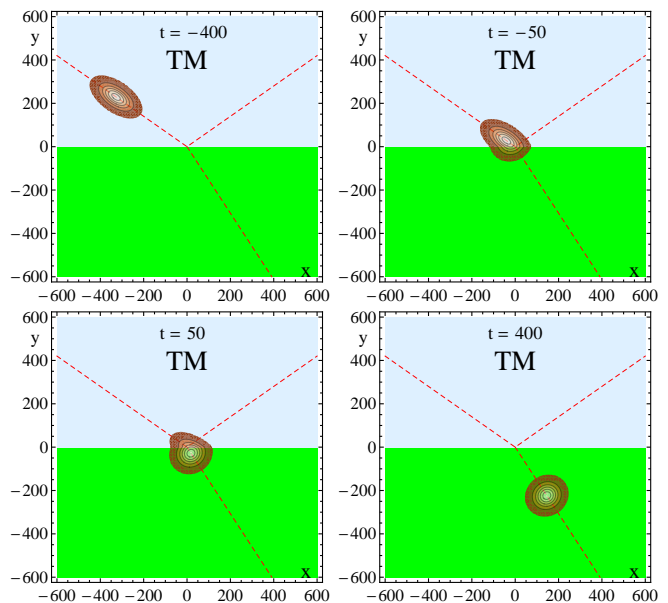


FIG. 2. (Color online) Results for $\mathcal{E}_{\text{TM}}(x, y, t)$, $t = -400, -50, 50$ and 400 , $\epsilon = 2.25$, $\mu = 1$, $\varphi_i = 55^\circ$, $w_{x_i} = 50$, $w_{y_i} = 100$. No noticeable reflection.

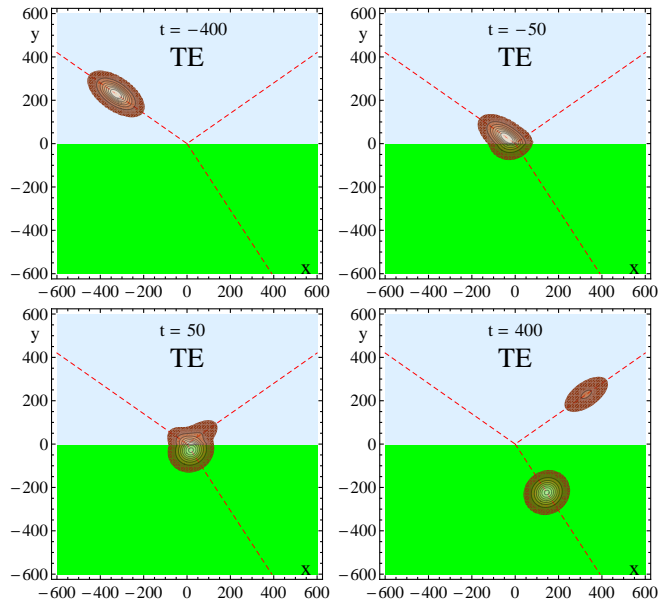
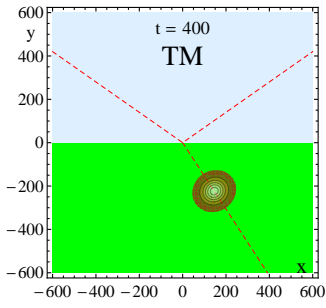
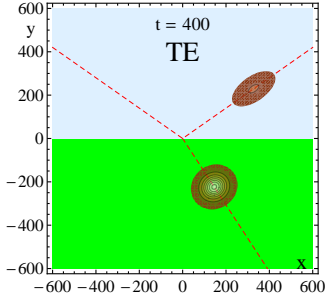


FIG. 3. (Color online) As in Fig. 2 but for $\mathcal{E}_{\text{TE}}(x, y, t)$ spatially averaged over the interference peaks.

laser pulse radii w_{x_i} and w_{y_i} by some factor a , the initial shapes in question will be expanded a times. If we multiply by a also the initial time $t_{\text{in}} (< 0)$, the initial shapes will be identical to ours shown in Figs. 2 and 3 at $t = -400$ (expanded a times). At the same time, the interference peaks which will be formed when the incident pulse reaches the interface, will be the same as ours ($a = 1$). This means that the plots for $a \neq 1$ can be obtained from those shown in Figs. 2 and 3, if one mul-



Video 1. (Color online) Time evolution for \mathcal{E}_{TM} shown in Fig. 2.



Video 2. (Color online) Time evolution for \mathcal{E}_{TE} shown in Fig. 3.

tiplies by a the numerical values associated with t and with the x and y axes (only the interference peaks will get squeezed a times). For the laser used in [1] (532 nm, 7 ps pulse duration, see p.75 right column), $a \simeq 20$.

Notice that the LHS of (8) gains the factor a^{-2} if y and w are multiplied by a . This increases the accuracy of (1) if $a > 1$.

In our case ($a = 1$),

$$\lambda_{\text{sw}} = 0.8717, \quad \frac{y_i^2(t = -400)}{\hat{y}_{x_i}^2} \approx 2.6 \times 10^{-3}, \quad (19)$$

and the applicability condition (2) implies $a_{\text{min}} \simeq 0.1$ ($w_{x_i \text{ min}} \simeq 5$). If $w_{y_i}/w_{x_i} = 2$ [1], this would imply $w_{y_i \text{ min}} \simeq 10$. However, the actual limitations on w_{y_i} result from the fact that this radius defines the laser pulse duration, $\tau_i = 2w_{y_i}$ (for $c = 1$).

In Fig. 4 we present the details of the interference peaks evolution.

A strong validity test for our formulas and calculations was a numerically confirmed continuity of the tangential components of \mathbf{E} and \mathbf{H} across the boundary ($y = 0^\pm$), and the fact that the total energy was conserved (time independent):

$$\int_{-1000}^{1000} dx \int_{-1000}^{1000} dy \mathcal{E}_{\text{TM}}(x, y, t) = 7853.982, \quad (20)$$

for any $t \in [-400, 400]$, and exactly the same result for $\mathcal{E}_{\text{TE}}(x, y, t)$, see Figs. 2 and 3. Incidentally, this conser-

vation was also valid for \mathcal{E}_{TM} and \mathcal{E}_{TE} spatially averaged over the interference peaks.

All calculations, figures, and videos were done by using *Mathematica*.

* zakow@ifpan.edu.pl

† andrzej.skorupski@ncbj.gov.pl

[1] L. Gao, J. Liang, C. Li, and L. V. Wang, *Nature* **516**, 74 (2014).

[2] P. F. Goldsmith, "Quasioptical systems: Gaussian beam, quasioptical propagation and applications," (IEEE Press/Chapman and Hall Publishers Series on Microwave

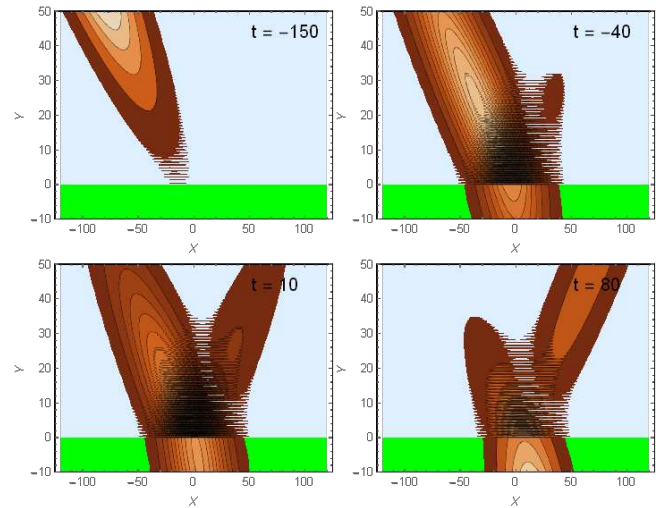


FIG. 4. (Color online) Results for $\mathcal{E}_{\text{TE}}(x, y, t)$, $t = -150, -40, 10$ and 80 , $w_{x_i} = 20$, and other parameters as in Fig 2.

- Technology and RF, New York, 1998) Chap. 2.
- [3] F. Scheck, "Classical field theory," (Springer, Heidelberg, Dordrecht, London, New York, 2012) Chap. 4.
- [4] J. D. Jackson, "Classical electrodynamics," (Wiley, New York, 1999) Chap. 7, 3rd ed.